Applied Computer Science, vol. 14, no. 3, pp. 43–53
doi:10.23743/acs-2018-20

Submitted: 2018-04-13
Revised: 2018-05-21
Accepted: 2018-09-03

deep-drawing, finite element method, sheet metal forming

Damian KRASKA[*], *Tomasz TRZEPIECIŃSKI*[*]

FINITE ELEMENT BASED PREDICTION OF DEFORMATION IN SHEET METAL FORMING PROCESS

Abstract

In this paper the sheet forming process of cylindrical drawpieces was simulated based on the finite element method by the explicit approach in the presence of contact conditions with isotropic and anisotropic friction. The experimental and numerical results obtained in the Abaqus finite element (FE) based program are presented. The aim of the experimental study is to analyse material behaviour under deformation and in addition to use the results to verify numerical simulation results. It was found that, although, the anisotropy of resistance to friction affects the height of ears, the influence of the friction formulation is relatively small in comparison with material anisotropy. The study indicates that FE analysis with 3-node triangular shell element S3R elements ensures the best approximation of the numerical results to the real process when both material and friction anisotropy are taken into account.

1. INTRODUCTION

The sheet forming process of complicated shell elements allows the production of thin walled parts. The design and analysis of sheet metal forming operations requires knowledge of the deformation mechanisms, material properties and boundary conditions (Affronti & Merklein, 2018; Hattalli & Srivatsa, 2018). The analytical analysis of the forming process is very complicated due to the strong nonlinear nature of the numerical procedures. For this reason,

[*] Rzeszow University of Technology, Faculty of Mechanical Engineering and Aeronautics, al. Powst. Warszawy 8, 35-959 Rzeszów, tel.: 17865 1714, e-mail: kraska94@gmail.com, tomtrz@prz.edu.pl

numerical modelling based on the finite element method (FEM) is currently a widely used approach because it ensures the simulation of a large number of parameters over a short duration.

The accuracy of the numerical results depends on several parameters including the types of finite mesh, material model of the yield criterion, and boundary conditions. The correctness of the material model and correctness of the experimental determination of material properties are two of the most important elements in modelling of FE data. The type of elements (shell, solid) decides on the representation of the contact conditions with moderate computing time. For the analysis of forming thin walled structures, shell elements are mostly used (Falsafi, Demirci & Silberschmidt, 2016; Ramzi, Sebastien, Fabrice, Gemala & Pierrick, 2017). When a material exhibits anisotropic properties, i.e., the value of the material parameters depends on the orientation according to the rolling direction of the sheet, an incorrect selection of the yield criterion does not reflect the complex material behaviour. The distortion of the yield surface shape due to the microstructural state of the material is named as plastic anisotropy (normal or planar). In planar anisotropy the properties vary with the orientation in the sheet plane. In normal anisotropy the properties differ in the direction of sheet thickness. Various approaches have emerged for developing the anisotropic yield criteria. A review and description of many proposals for anisotropic yield criteria has been prepared by e.g.. Banabic (2010).

In this paper the results of experiments and numerical simulations of forming cylindrical cups are presented. The aim of the experimental study is to analyse the material behaviour under deformation and further use the results to verify numerical simulation results. In FE models, the mesh density, the number of elements and the type of material and the friction model are taken into account.

2. EXPERIMENTAL

2.1. Material

The drawpieces analysed in this paper were manufactured from deep drawing 1-mm-thick steel sheet DC04. The basic mechanical parameters of this material were determined in the uniaxial tensile test according to the procedure described in the PN-EN ISO 6892-1:2010 standard. The specimens for the tensile test were cut at angles of 0°, 45° and 90° with respect to the rolling direction of the sheet metal. The following parameters were determined (Table 1): the ultimate tensile strength R_m, field stress $R_{p0,2}$, elongation A_{50}, strain hardening exponent n, strain hardening coefficient K, and Lankford's (anisotropy) coefficient r. Five specimens were tested for three orientations (0°, 45° and 90°), and the average values of specific parameters were determined.

Tab. 1. Basic mechanical properties of DC04 steel sheet

Sample orientation	$R_{p0.2}$, *MPa*	R_m, *MPa*	A_{50}	*C*, *MPa*	*n*	*r*
0°	176	301	0.42	500	0.19	1.81
45°	180	293	0.39	497	0.17	1.88
90°	192	315	0.41	477	0.17	1.4

2.2. Method

The cylindrical drawpieces were fabricated using a special device shown in Fig. 1. The drawpieces were formed from discs with diameters of 56 mm. To prevent wrinkling of the drawpiece flange, a blankholder was applied. In the stamp-ing tool, the blankholder pressure is forced by screwing the pressure plate onto the body using a torque wrench. An increase of moment at the torque wrench at about M = 15 Nm causes an increase of normal pressure force at P_{bd} = 1 kN. The diameter of the cylindrical punch is 29.3 mm. The diameter of the hole in the die is 32.3 mm. The edges of die and punch were rounded with a radius of 3 mm. The complete drawing operation was conducted using the hydraulic test machine at room temperature.

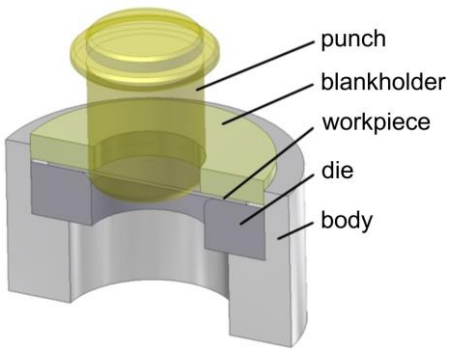

Fig. 1. Schematic of stamping tool

The results of numerical modelling were verified on the basis of meas-urements of the wall thickness of the drawpieces in characteristic locations (Fig. 2a). The drawpieces were cut along the rolling direction of the sheet using a me-chanical metal saw (to minimise the influence of heat on the cross-sectional structure of the material). Then the cutting surface was ground using sandpaper with P80, P200, P800 and P2000 grains. The measurement of wall thickness of the drawpieces based on the sectional photos of thickness variation (Fig. 2b) made by Alicona's InfiniteFocusG4.

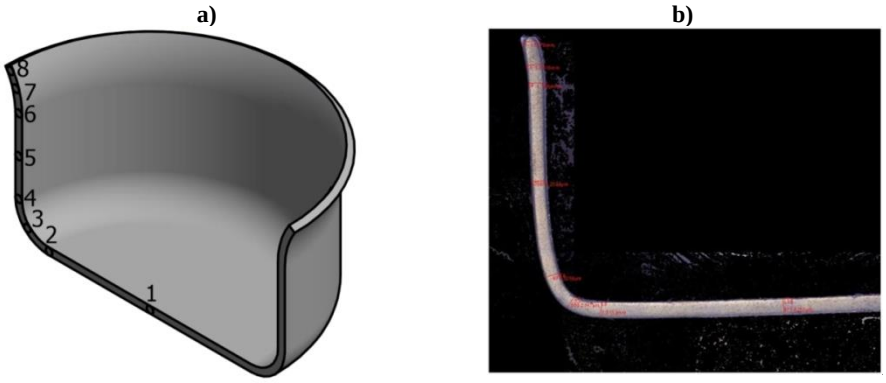

Fig. 2. a) The location of the characteristic locations for detection of thickness measurements and b) an typical picture of drawpiece section

3. NUMERICAL MODELING

A 3D numerical model of the drawpiece forming was built in Abaqus 6.14-5 finite element code used for the computer aided analysis of sheet metal forming processes (Li et al., 2017; Trzepieciński & Gelgele, 2011). The geometry of the tools and sheet in the numerical simulation (Fig. 3) corresponds to the experimental setup shown in Fig. 1.

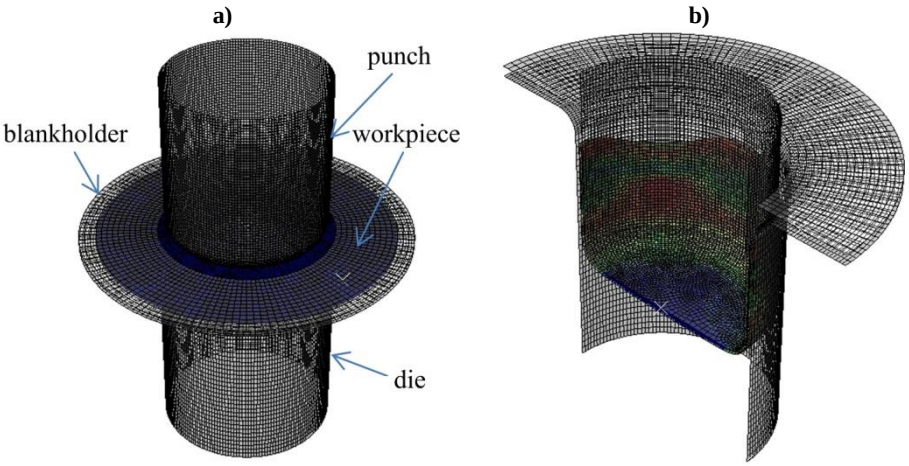

Fig. 3. Numerical model of the stamping process: a) initial stage and b) final stage of forming

The surface of tools was discretised using 4-node bilinear rigid quadrilateral R3D4 shell elements. To find the optimal parameters of the numerical model, the following parameters were considered:

- mesh density: 4475, 11160, 30876 elements,
- element type: S3R, S4, S4R, S4RS,
- material model: isotropic, anisotropic,
- friction model: isotropic, anisotropic.

An elastic-plastic material model approach was implemented and two material models have been simulated. In the case of the first isotropic material behaviour approach the von Mises yield criterion (von Mises, 1913) is used. In the second numerical model, the anisotropy of the material has been established using Hill's (1948) yield criterion which is commonly used for the material description of steel sheet metals. The Hill (1948) formulation is an extension of the isotropic von Mises function, and can be expressed in terms of rectangular Cartesian stress components as:

$$\bar{\sigma} = \sqrt{F(\sigma_{22} - \sigma_{33})^2 + G(\sigma_{33} - \sigma_{11})^2 + H(\sigma_{11} - \sigma_{22})^2 + 2L{\sigma_{23}}^2 + 2M{\sigma_{31}}^2 + 2N{\sigma_{12}}^2} \quad (1)$$

where $\bar{\sigma}$ is the equivalent stress, and indics 1, 2, 3 represent the rolling, transverse and normal directions to the sheet surface. The constants F, G, H, L, M and N define the anisotropic state of the material and are equal to:

$$F = \frac{1}{2}\left(\frac{1}{{R_{22}}^2} + \frac{1}{{R_{33}}^2} - \frac{1}{{R_{11}}^2}\right),\ G = \frac{1}{2}\left(\frac{1}{{R_{11}}^2} + \frac{1}{{R_{33}}^2} - \frac{1}{{R_{22}}^2}\right),\ H = \frac{1}{2}\left(\frac{1}{{R_{11}}^2} + \frac{1}{{R_{22}}^2} - \frac{1}{{R_{33}}^2}\right),$$
$$L = \frac{3}{2{R_{23}}^2},\ M = \frac{3}{2{R_{13}}^2},\ N = \frac{3}{2{R_{12}}^2} \quad (2)$$

The parameters R_{11}, R_{22}, R_{33}, are defined in ABAQUS from user input consisting of ratios of yield stress in different directions with respect to a reference stress. The elastic properties of the sheet are specified using the following properties: Young's modulus: E = 2.1 GPa, Poisson's ratio ν = 0.3. The mass density was ρ = 7860 kg·m^{-3}. The isotropic hardening behaviour implemented in the numerical model uses the Hollomon power-type law:

$$\sigma = K\varphi^n \quad (3)$$

with the parameters specified in Table 1.

Five integration points through the thickness direction are employed. This number of integration points through the shell thickness is sufficient for an acceptable solution (Larsson, 2009). The *explicit* direct integration available from Abaqus is used in the model to handle nonlinearity from large displacements, material non-linearity and boundary non-linearity such as contact, sliding and friction.

In the *explicit* procedure, the displacements, velocities and accelerations of each node are advanced explicitly through time. This means that the state of the model at the end of time $t+\Delta t$ is solely based on the displacements, velocities and accelerations at the beginning of time t.

To describe the contact conditions between sheet and tools, the classical friction model following Coulomb's law is assumed, in which the relationship between frictional stresses τ and normal stresses σ may be expressed as:

$$\tau = \mu\sigma \tag{4}$$

The anisotropic elliptical friction model was implemented by specifying different friction coefficients in the two orthogonal directions on the contact surface. To use an anisotropic friction model built in Abaqus, the two friction coefficients (0.12 and 0.15) were specified. The methodology and device for determination anisotropic friction coefficient have been described in the previous paper of authors (Trzepieciński & Gelgele, 2011). In the isotropic friction model, the average friction coefficient 0.135 was specified.

3. RESULTS AND DISCUSSION

As regards the effect of the type of finite element on the accuracy of predicting the thickness changes of the drawpiece wall (Fig. 2a), the best approximation of experimental data was observed for elements of the S3R type (Fig. 4). The smallest value of the errors of thickness prediction is observed on the upper edge of the drawpiece (point 8 in Fig. 4). The sheet thickness distributions presented in Fig. 4 relate to a drawpiece formed from a disc with a diameter of 56 mm.

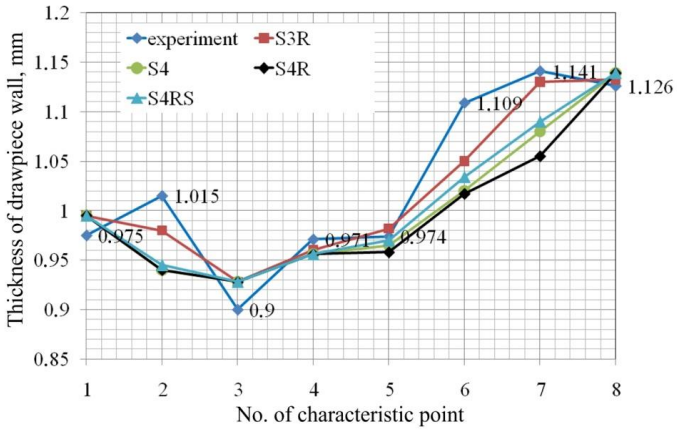

Fig. 4. Distribution of wall thickness of a cylindrical drawpiece along the sheet rolling direction

The type of finite element has a significant effect in determining the duration of the calculation. The calculation time for a model containing the elements of S4 type is almost five times greater than for the simulation of a blank model discretised with the elements of the S3R type (Fig. 5). The distributions of wall thickness of the drawpieces shown in Fig 6, indicate that although the type of element significantly affects the calculation time, both the distribution, the value of the maximum wall thickness and its location of occurrence, according to Fig. 2a, are very similar for the types of elements analysed.

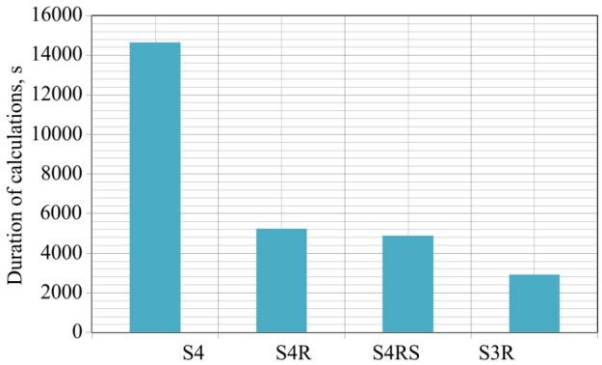

Fig. 5. Duration of calculation for specific types of finite elements

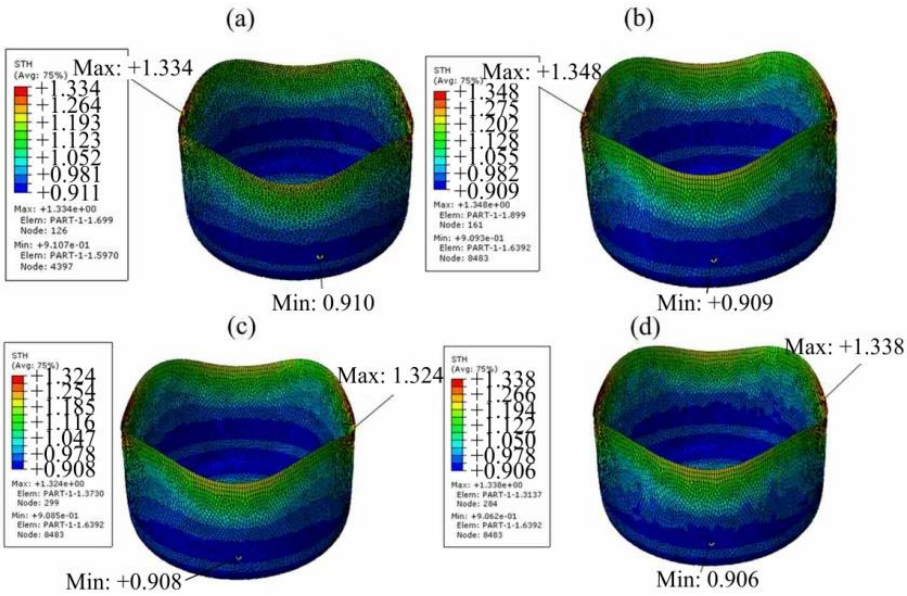

Fig. 6. Distribution of wall thickness of a drawpiece in relation to element type: a) S3R b) S4 c) S4R d) S4RS

As previously shown, the best approximation of experimental data is ensured by the use of S3R type elements, for which an analysis was performed which examined the impact of the material model and the friction model on the change of the wall thickness distribution (Fig. 7). Taking the isotropic properties of the material in the numerical model into account in combination with both models of friction causes a significant overestimation of the wall thickness of the drawpiece in the area of the flange (Fig. 7). The best adaptation of the numerical data to the experimental data is clearly visible for (i) the zone of the cylindrical side wall, (ii) the edge of the drawpiece and (iii) the point located in the middle of the bottom of the drawpiece.

The best prediction of the maximum force of drawpiece forming in comparison with the experimentally recorded data (26.5 kN) provides a numerical model which takes into account the anisotropy of the material and the isotropy of changes in the coefficient of friction (Fig. 8).

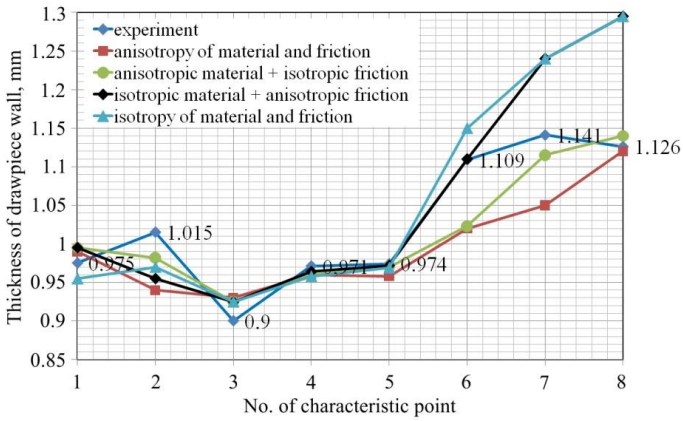

Fig. 7. Effect of both the material and friction model on the distribution of the thickness of an axisymmetric drawpiece

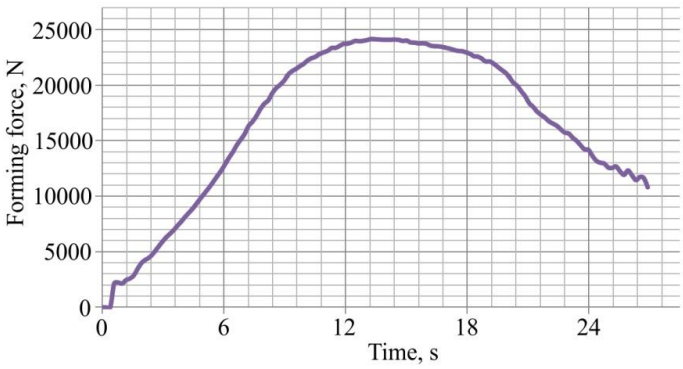

Fig. 8. Distribution of the forming force for an anisotropic model of the material and isotropy of friction

The material model adopted (isotropic, anisotropic) has a crucial influence on the value of the forming force. Additional consideration of the nature of changes in the coefficient of friction (isotropy, anisotropy) affects the change in the value of the forming force to lesser extent. Taking into account the anisotropy of both factors studied (friction and material) requires more computing power and is the most time consuming. (Fig. 9).

Material anisotropy is the decisive factor from the point of view of the ability to simulate the formation of the drawpiece ears (Fig. 10).

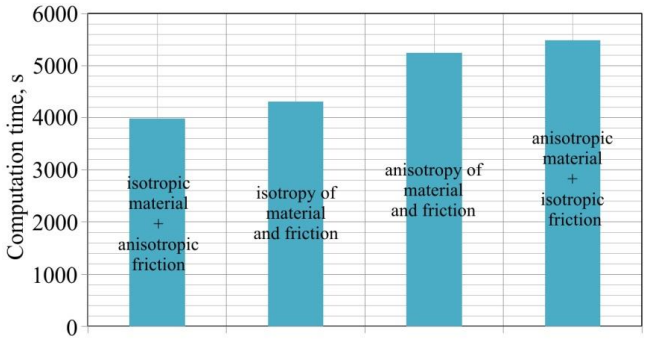

Fig. 9. Effect of friction and material model configurations on the computation time

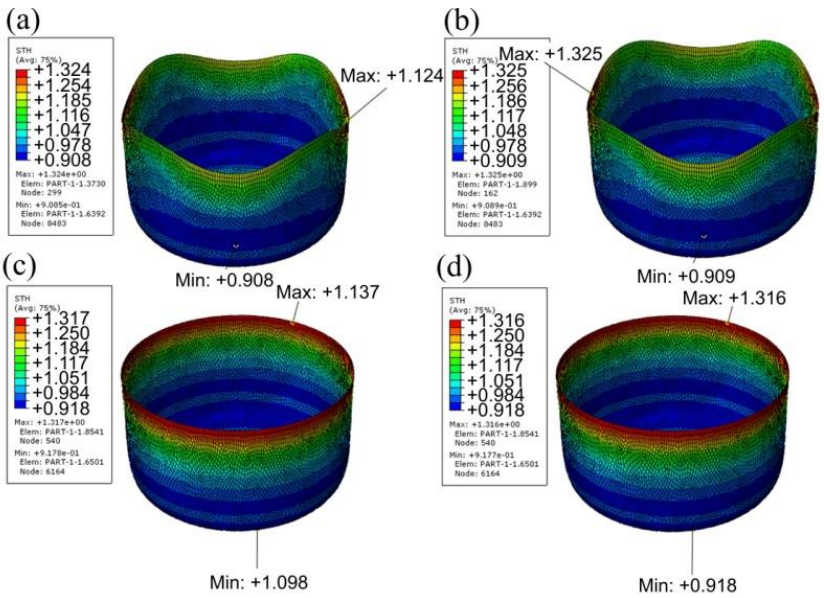

Fig. 10. The distribution of wall thickness of a cylindrical drawpiece under different modelling strategies: (a) anisotropy of both material and friction, (b) anisotropy of material and isotropy of friction, (c) isotropic material and frictional anisotropy, (d) isotropy of both material and friction

The assumption of an anisotropic friction model, coupled with the isotropic model of the material, does not provide an accurate prediction of material flow consistent with the experiment. The height of the drawpiece is very similar on the perimeter of the cup. Therefore, it can be concluded that the assumption of an anisotropic model of the material with frictional isotropy is a more correct solution than the inverse situation that takes into account the isotropic model of the material with frictional anisotropy.

3. SUMMARY AND CONCLUSIONS

The analysis of sheet metal forming requires the taking into account of non-linear phenomena, i.e. material non-linearity including the strain hardening phenomenon, and boundary conditions. The investigations of many research projects are focused on a suitable selection of the material model. However, the research on forming cylindrical cups presented in this paper confirms that to accurately predict the material flow, frictional anisotropy should be also taken into account. Although, the anisotropy of resistance to friction affects the height of ears, the influence of the friction formulation is relatively small in comparison with material anisotropy. An explicit procedure used to handle nonlinearity from large displacements, material non-linearity and boundary non-linearity shows that a large-strain 3-node triangular shell element S3R, which is a degenerated version of an S4R shell element, ensures the best prediction of the thickness of the drawpiece wall. In the future, analysis will be carried out of the prediction of material flow of different anisotropic materials and friction models.

REFERENCES

Affronti, E., & Merklein, M. (2018). Analysis of the bending effects and the biaxial pre-straining in sheet metal stretch forming processes for the determination of the forming limits. *International Journal of Mechanical Sciences, 138–139*, 295–309. doi:10.1016/j.ijmecsci.2018.02.024

Banabic, D. (2010). S*heet metal forming processes. Constitutive modelling and numerical simulation*. Berlin Heidelberg: Springer-Verlag.

Falsafi, J., Demirci, E., & Silberschmidt, V. V. (2016). Computational assessment of residual formability in sheet metal forming processes for sustainable recycling. *International Journal of Mechanical Sciences*, *119*, 187–196. doi:10.1016/j.ijmecsci.2016.10.013

Hattalli, V. L., & Srivatsa, S. R. (2018). Sheet metal forming processes – recent technological advances. *Materials Today – Proceedings*, *5*(1), 2564–2574. doi:10.1016/j.matpr.2017.11. 040

Hill, R. (1948). A theory of the yielding and plastic flow of anisotropic metals. *Proceedings of the Royal Society A*, *193*, 281–297. doi:10.1098/rspa.1948.0045

Larsson, M. (2009). Computational characterization of drawbeads: A basic modelling method for data generation. *Journal of Materials Processing Technology*, *209*(1), 376–386. doi:10.1016/ j.jmatprotec.2008.02.009

Li, P., He, J., Liu, Q., Yang, M., Wang, Q., Yuan, Q., & Li, Y. (2017). Evaluation of forming forces in ultrasonic incremental sheet metal forming. *Aerospace Science and Technology*, *63*, 132–139. doi:10.1016/j.ast.2016.12.028

Ramzi, B. H., Sebastien, T., Fabrice, R., Gemala, H., & Pierrick, M. (2017). Numerical prediction of the forming limit diagrams of thin sheet metal using SPIF tests. *Procedia Engineering*, *183*, 113–118. doi:10.1016/j.proeng.2017.04.029

Trzepieciński, T., & Gelgele, H. L. (2011). Investigation of anisotropy problems in sheet metal forming using finite element method. *International Journal of Material Forming*, *4*(4), 357–369. doi:10.1007/s12289-010-0994-7

von Mises, R. (1913). Mechanik der festen Kö¨rper im plastisch deformablen Zustand. *Nachrichten von der Köngl. Gesellschaft der Wissenschaften zu Göttingen, Mathematisch-Physikalische Klasse 1913*, 582–592.